Turk J Chem
36 (2012) , 147 – 158.

doi:10.3906/kim-1105-40

A DFT study on the structural and optical properties and cation selectivities of some metal-coumarin-crown ether complexes

Emine Esra KASAPBAŞI, Mine YURTSEVER*
Department of Chemistry, İstanbul Technical University,
Maslak 34469, İstanbul-TURKEY
e-mail: mine@itu.edu.tr

Received: 17.05.2011

Macrocyclic ethers are well-known molecules because of their high cation-binding capacities. They form stable complexes with alkaline and soil alkaline metals through strong oxygen bridges in solution. For enhanced optical properties, a new series of crown ethers was synthesized with a coumarin ring fused to it. The effects of the position of the coumarin ring, the type of the substituent on the coumarin ring, and the size of the crown on the optical properties of the material were studied according to the density functional theory (DFT) method at the B3LYP/6-31g(d) level of theory in the gas phase as well as in the solvent medium. The ion selectivities of different coumarin-crown ether molecules were also studied by calculating the metal-binding energies at the same level of theory. The excited-state electronic energies were calculated by using the time-dependent density functional theory (TDDFT) method, and the theoretical UV absorption spectra of the studied molecules were plotted and compared to the experimental spectra if available.

Key Words: Coumarin, crown ethers, UV, density functional theory, time-dependent density functional theory

Introduction

Crown ethers[1,2] have been drawing attention due to their ability of binding metal cations in solution. They have a very wide range of industrial as well as biological applications. They have become a model for biologically important host-guest interactions, and their practical utility can be found in the areas of chromatography,

*Corresponding author

separation, molecular transport, catalysis, selective transport and separation of metals, phase-transfer catalysis, solvation of ions in nonpolar solvents, stabilization of proton action sites in biological molecules, and isolation of radioactive components of nuclear wastes.[3–5] There are many aspects of crown ethers that determine selectivity, such as the size of the macrocycle and the nature and arrangement of the donor groups.[6]

The coumarins of benzopyran are important π-conjugated compounds that are extracted from natural plants. They are important molecules due to their chromophoric properties.[7] To combine the optical features of the coumarin derivatives with the selective cation-binding features of macrocyclic crown ethers, a series of new molecules was synthesized by Tiftikçi and Erk.[8] Since they can dissolve in free or complex form, coumarin-crown ethers could be used as phase-transfer carriers or liquid membrane systems. Crown ethers form a stable complex with metal cations in the solid state and their decomposition temperatures are over 200 °C, whereas coumarin derivatives of crown ethers are soluble in common solvents like $CHCl_3$ and CH_2Cl_2 and can serve as good cation extractors in aqueous media.[9] It is known that the metal cation selectivity of crown ethers in solution is highly related to the size match between the metal cation and the crown cavity. However, size matching may not be the only factor affecting the metal-ion binding energies measured in the gas phase.[10,11] In this study, effects of factors other than the size of the crown on the metal-binding energies, such as the type and the place of the substituent group on the coumarin ring and the fusion position of the coumarin ring to crown ether, as well as the effects on the optical properties, were investigated in the gas phase and also in acetonitrile.

Method

The molecules were divided into 2 categories, as series 5 and 6, depending on the attachment position of the coumarin ring to the crown ring. In series 5, the attachment to the carbon atom occurs at position 3 with respect to the oxygen atom, whereas, in series 6, it occurs at position 2 (Figure 1). The letters a, b, and c are used to denote that the substituents are methyl and ethyl, and the letters d, e, and f are used to denote that the substituent is n-propyl. The numbering of the crown oxygen atoms and all other atoms are shown for 6c (Figure 2), and the number coding of all molecules is given in Table 1.

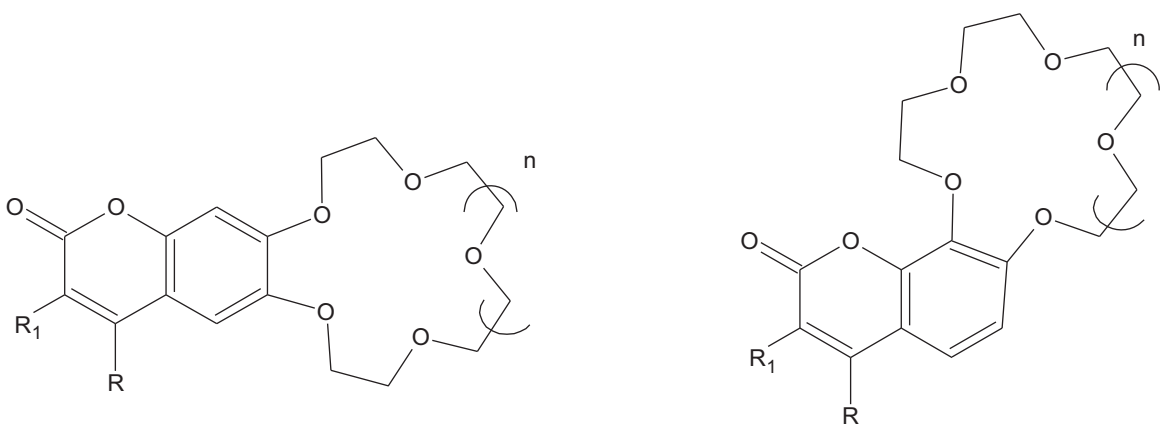

Figure 1. Coumarin-crown ether molecule: series 5 (left) and series 6 (right).

The geometries of the studied coumarin-crown ether molecules were optimized by the density functional theory (DFT)[12,13] method, using the B3LYP hybrid functional[14] with the 6-31g(d)[15] basis set implemented

in the Gaussian 2003 software package.[16] The geometries presented here are lowest-energy stationary states confirmed by the all-positive vibrational frequencies. For the optical properties, the excited states were optimized by the time-dependent DFT (TDDFT) method,[17−19] and the UV absorption frequencies corresponding to the electronic transitions were obtained. The solvent effect was studied at the same level of theory by the integral equation formalism polarized continuum model (IEF-PCM)[20] method, which gives an accurate description of the electrostatic interaction between the solute and the solvent modeled in terms of an apparent surface charge spread on a cavity of molecular shape. The theoretical UV spectra were obtained by fitting a Gaussian curve with a band width of 200 nm to each UV absorbance frequency. The shifts in the spectral peaks due to the coordination of a metal, the size of the crown ring, the type and position of the substituents on the coumarin, and the position of the coumarin ring were then analyzed. The presented binding energies were basis set superposition error (bsse) corrected energies calculated by the counterpoise method with the enlarged basis sets of 6-31+g(d).

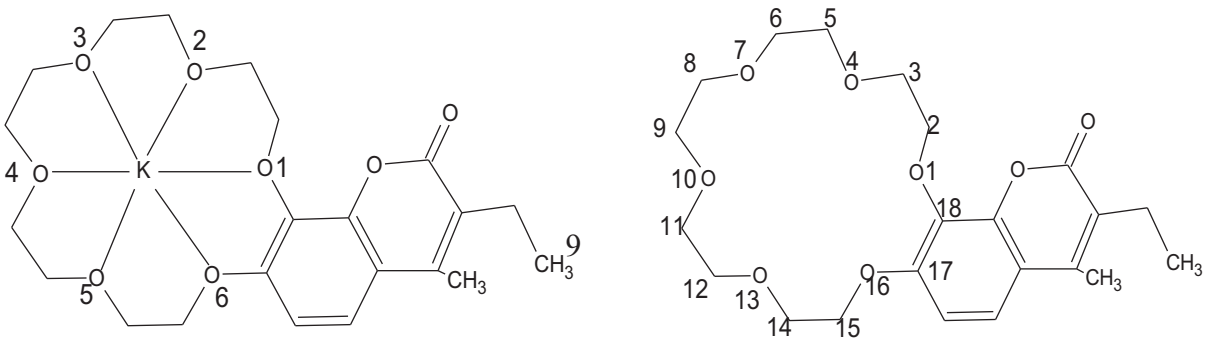

Figure 2. The numbering of crown oxygens and all atoms in 6c.

Table 1. Number coding of the studied molecules.

Code	n	R	R_1	Code	N	R	R_1
5a	0	$-CH_3$	$-C_2H_5$	**6a**	0	$-CH_3$	$-C_2H_5$
5b	1	$-CH_3$	$-C_2H_5$	**6b**	1	$-CH_3$	$-C_2H_5$
5c	2	$-CH_3$	$-C_2H_5$	**6c**	2	$-CH_3$	$-C_2H_5$
5d	0	$-C_3H_7$	-H	**6d**	0	$-C_3H_7$	-H
5e	1	$-C_3H_7$	-H	**6e**	1	$-C_3H_7$	-H
5f	2	$-C_3H_7$	-H	**6f**	2	$-C_3H_7$	-H

Results and discussion

Structural properties

The optimized geometries of $18c6Na^+$ (Table 2)[21] and $18c6K^+$ (Table 3)[22] molecules were compared to the X-ray data. Although some of the dihedral angles seemed mismatched, the structure was still the same. The same difference between the experimental and theoretical dihedral angle of C_3-O_4-C_5-C_6 was also observed in the

dihedral angle of C_{12}-O_{13}-C_{14}-C_{15}, but in an opposite manner. Due to the symmetric nature of the molecule, either group may have the possibility of deviating from planarity. The existence of 3 energetically degenerate conformations having different symmetries, such as D_{3d}, C_{3v}, and C_1 for 18c6-metal ion complexes, was also reported very recently in the literature.[23] The good agreement between experimental and theoretical geometric parameters shows that the optimized geometries are reliable and can be further used in binding-energy and optical-property calculations.

Table 2. Comparison of the experimental (X-ray)[21] and theoretical (DFT) geometric parameters of $18c6Na^+$.

Atom	Distance (Å)		Angle (°)		Dihedral angle (°)	
a-b-c-d	b-c		a-b-c		a-b-c-d	
	Exp.	This work	Exp.	This work	Exp.	This work
C(18)-O(1)-C(2)-C(3)	1. 42	1. 43	112. 2	112. 8	173. 0	162. 5
O(1)-C(2)-C(3)-O(4)	1. 50	1. 51	107. 6	108. 4	60. 7	–59. 1
C(2)-C(3)-O(4)-C(5)	1. 41	1. 43	108. 5	107. 4	–171. 3	–168. 8
C(3)-O(4)-C(5)-C(6)	1. 43	1. 43	111. 4	114. 7	–177. 4	–71. 8
O(4)-C(5)-C(6)-O(7)	1. 50	1. 52	108. 5	112. 0	–59. 4	–53. 5
C(5)-C(6)-O(7)-C(8)	1. 42	1. 42	107. 7	107. 4	–172. 6	173. 0
C(6)-O(7)-C(8)-C(9)	1. 41	1. 43	111. 9	113. 2	–176. 9	166. 5
O(7)-C(8)-C(9)-O(10)	1. 51	1. 51	107. 7	108. 1	52. 4	57. 7
C(8)-C(9)-O(10)-C(11)	1. 42	1. 42	112. 4	108. 9	70. 5	–175. 7
C(9)-O(10)-C(11)- C(12)	1. 43	1. 42	113. 9	111. 6	–172. 3	175. 7
O(10)-C(11)- C(12)-O(13)	1. 49	1. 51	108. 2	108. 9	63. 4	–57. 7
C(11)- C(12)-O(13)-C(14)	1. 44	1. 43	106. 0	108. 1	–176. 0	–166. 5
C(12)-O(13)-C(14)-C(15)	1. 42	1. 42	114. 1	113. 2	76. 8	–173. 0
O(13)-C(14)-C(15)-O(16)	1. 51	1. 52	113. 6	107. 4	46. 6	53. 5
C(14)-C(15)-O(16)-C(17)	1. 43	1. 43	111. 6	112. 0	114. 7	71. 8
C(15)-O(16)-C(17)-C(18)	1. 43	1. 43	116. 5	114. 7	–73. 7	168. 8
O(16)-C(17)-C(18)-O(1)	1. 51	1. 51	112. 1	107. 4	–58. 5	59. 1
C(17)-C(18)-O(1)-C(2)	1. 42	1. 43	107. 1	108. 4	166. 5	–162. 5

Optical properties

In Figure 3, the experimental and theoretical UV spectra obtained for the 5e and 6b molecules in the absence of a metal ion (Figure 4) are shown. Theoretical spectra were drawn in the gas phase as well as in acetonitrile (ε = 37.5). Experimental spectra were also obtained in the same solvent. There were slight differences between the experimental and theoretical absorption peak maxima corresponding to the $\pi - \pi^*$ transition of the aromatic rings. The theoretical λ_{max} was obtained at a higher wavelength by approximately 30 nm in 5e, whereas it was obtained at a lower wavelength by approximately 15 nm in 6b, when compared to the experimental results in acetonitrile. These molecules showed opposite trends due to differences in their planarity and the π-electron density in the coumarin moiety, whose stability also affects the geometry of the crown moiety. The

studied molecules are sensitive to the polarity of the medium since the peak maxima of both molecules showed bathochromic shifts in acetonitrile, which is a highly polar solvent and may change the stability of the coumarin moiety. The resemblance of the theoretical and the experimental spectra and the fairly good agreement in the wavelengths of the absorption peaks allowed us to study the optical properties of the other molecules in the series.

Table 3. Comparison of the experimental (X-ray)[22] and theoretical (DFT) geometric parameters of $18c6K^+$.

Atoms	Distance (Å)		Angle (°)		Dihedral angle (°)	
a-b-c-d	b-c		a-b-c		a-b-c-d	
	Exp.	This work	Exp.	This work	Exp.	This work
C(9)-O(1)-C(2)-C(3)	1. 42	1. 43	112. 9	113. 2	–170. 8	175. 1
O(1)-C(2)-C(3)-O(4)	1. 50	1. 51	108. 1	109. 3	–65. 2	64. 2
C(2)-C(3)-O(4)-C(5)	1. 41	1. 43	108. 9	108. 5	178. 9	171. 1
C(3)-O(4)-C(5)-C(6)	1. 42	1. 43	111. 6	115. 1	178. 1	82. 5
O(4)-C(5)-C(6)-O(7)	1. 51	1. 52	108. 2	113. 2	70. 0	60. 2
C(5)-C(6)-O(7)-C(8)	1. 42	1. 42	109. 4	108. 5	–175. 5	178. 4
C(6)-O(7)-C(8)-C(9)	1. 42	1. 42	112. 0	113. 2	–177. 4	–178. 0
O(7)-C(8)-C(9)-O(1)	1. 51	1. 51	108. 9	109. 1	–65.3	–63. 2
C(8)-C(9)-O(1)-C(2)	1. 42	1. 43	107. 5	109. 0	–177. 5	–175. 1

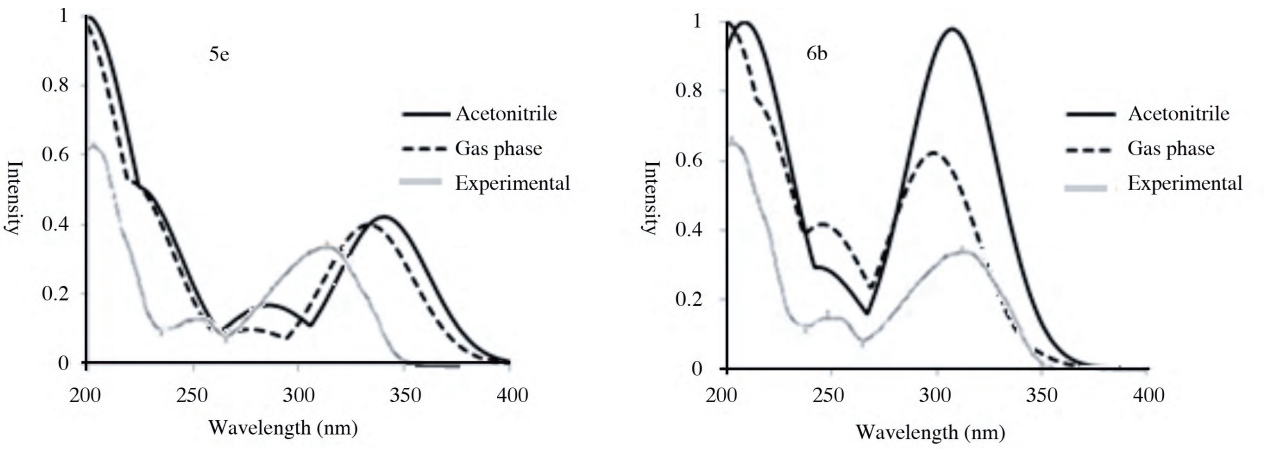

Figure 3. The theoretical and experimental UV spectra of 5e and 6b.

The optical properties of the crown ethers, which do not normally absorb light in the UV region, are improved by the incorporation of the coumarin part. The maximum absorption peaks for all studied molecules that showed blue or red shifts depending on the structure upon coordination of a metal ion are given in Table 4. The maximum peaks of crown ethers observed at wavelengths between 140 and 160 nm were shifted to higher wavelengths because of the stabilizing effects of the coumarin aromatic ring attached to them, and these peaks were observed at 190-220 nm. The second peaks appeared to vary between 200 and 320 nm depending on the size of the crown ethers, and they were highly affected by the type of the substituent and also by the type of the

metal cation. Red shifts in these peaks were observed if the crown ethers accommodated the metal ion better, as expected. The third peaks were less intense compared to the second ones and showed red shifts in series 5, in which the position of the substituent group enabled better π-electron delocalization on the aromatic rings.

Table 4. Maximum absorption wavelengths (in nm).

Molecule	No Metal			Li+			Na^+			K^+		
	λ_1	λ_2	λ_3	$\lambda 1$	$\lambda 2$	$\lambda 3$	λ_1	λ_2	λ_3	λ_1	λ_2	λ_3
5a	192	272	308	196	213	302	212	263	301	213	264	300
5b	191	277	328	206	215	301	196	273	308	217	278	328
5c	221	268	328	201	258	320	197	289	289	217	258	303
6a	191	212	291	197	-	291	201	215	292	217	-	292
6b	205	243	298	197	218	291	198	218	291	200	245	291
6c	194	241	295	199	246	275	181	256	274	184	201	264
5d	190	210	309	190	212	300	194	210	301	212	272	305
5e	191	279	333	194	281	328	198	262	328	261	212	311
5f	196	271	331	202	290	-	197	287	-	196	240	362
6d	191	-	292	200	273	293	198	269	291	215	-	292
6e	197	243	297	199	215	292	192	216	284	199	245	290
6f	194	241	295	181	199	275	202	281	306	182	256	277

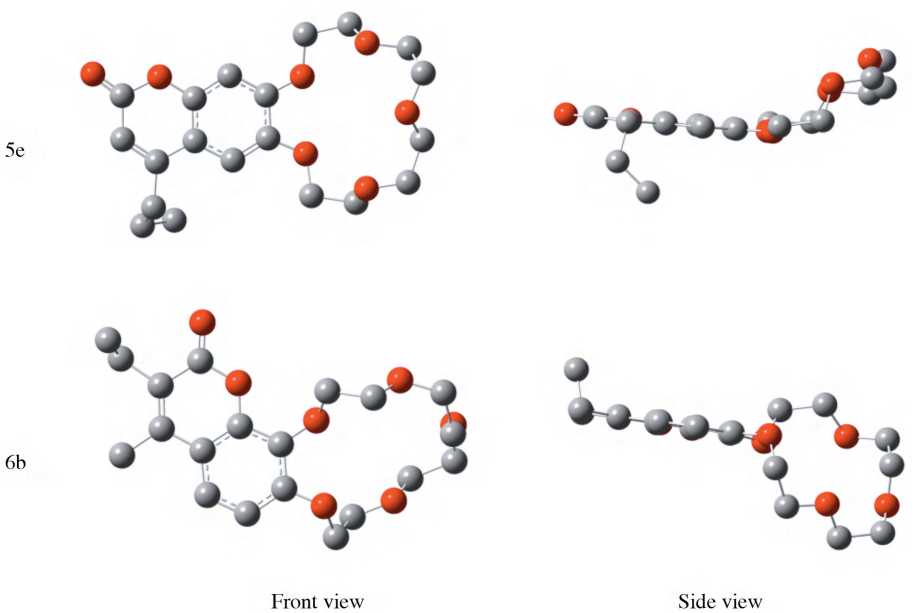

Figure 4. Different views of molecules 5e and 6b.

Cation selectivities

The bsse-corrected electronic energies of the Li^+-, Na^+-, and K^+-bearing coumarin-crown ether molecules were calculated at the B3LYP/6-31+g(d)//B3LYP/6-31g(d) level. Using these energies, the stabilization energies gained by the coumarin-crown ether molecules upon coordination of a metal ion or binding energies (ΔE) were calculated using Eq. (1), where M represents the metal cation and L represents the coumarin-crown ether molecule. The binding energies for all ML complexes are given in Table 5.

$$\Delta E = E_{ML} - (E_M + E_L) \tag{1}$$

The binding energy highly depends upon the size of the ion, the size of the crown cavity, and the substituent.[24] The Li^+ ion is accommodated better in 6e and 5b, the Na^+ ion is accommodated better in 5b and 6e, and the K^+ ion is accommodated better in the 6c, 5c, and 6f complexes. The effect of the substituent is different in series 5 and 6, and it is more pronounced if the size of the crown is small. The binding energies of all metal ions are larger for the 5a, 5b, and 5c complexes than for 6a, 6b, and 6c, whereas the opposite trend is observed for 5d, 5e, and 5f, whose metal-binding energies are smaller than those of 6d, 6e, and 6f . The 15c5 complexes are more affected by the type of the substituents and the position of the coumarin, since the crown ring contains an odd number of oxygen atoms, namely 5, and the ring is unsymmetrical. The difference between the maximum and minimum binding energy of a metal ion varies between 30 and 40 kcal/mol. The same difference was observed to change between 0.7 and 32.8 kcal/mol depending on the substituent or position of the coumarin.

Table 5. Binding energies (in kcal/mol) of Li^+, Na^+, and K^+.

Molecule	Li^+	Na^+	K^+	Molecule	Li^+	Na^+	K^+
5a	–86.6	–61.9	–35.5	**5d**	–72.4	–63.0	–36.2
5b	–100.0	–76.6	–49.2	**5e**	–83.1	–66.7	–41.3
5c	–85.6	–71.2	–61.6	**5f**	–88.8	–69.4	–41.0
6a	–73.3	–65.5	–38.8	**6d**	–74.7	–64.8	–38.1
6b	–71.3	–44.6	–24.1	**6e**	–103.9	–75.7	–56.9
6c	–95.8	–74.1	–64.9	**6f**	–94.7	–64.4	–62.2

The metal ions are located almost at the center of the crown cavity, and a strong coordination bond occurs between the positively charged center and the lone pair electrons of the crown oxygens. The metal ion and oxygen average distances are given in Table 6.

Due to the small size of the lithium ion, its average distance slightly increases as the size of the crown ring increases, whereas the average distances for the Na and K ions remain almost unchanged.

The coordination of the metal ions to the crown cavity and the metal-oxygen distances are shown in the 12c4 (Figure 5), 15c5 (Figure 6), and 18c6 (Figure 7) types of molecules. Good agreement between the experimental and theoretical bond distances in 18c6Na^+ and 18c6K^+ (Table 7) were observed.[25]

Table 6. Average (M^+-O) bond distances and the standard deviations (SD) (in Å).

	r_{M^+-O}	SD	r_{M^+-O}	SD	r_{M^+-O}	SD
	5a		**5b**		**5c**	
Li	2.00	0.026	2.08	0.026	2.22	0.153
Na	2.31	0.017	2.34	0.025	2.38	0.005
K	2.87	0.368	2.80	0.061	2.80	0.021
	5d		**5e**		**5f**	
Li	1.87	0.021	2.05	0.078	2.23	0.063
Na	2.32	0.013	2.33	0.019	2.38	0.004
K	2.78	0.176	2.73	0.021	2.79	0.020
	6a		**6b**		**6c**	
Li	1.98	0.039	2.08	0.049	2.23	0.056
Na	2.32	0.015	2.34	0.038	2.37	0.018
K	2.78	0.152	2.72	0.017	2.79	0.015
	6d		**6e**		**6f**	
Li	1.86	0.030	2.08	0.048	2.22	0.046
Na	2.32	0.017	2.34	0.040	2.36	0.045
K	2.76	0.146	2.72	0.013	2.80	0.036

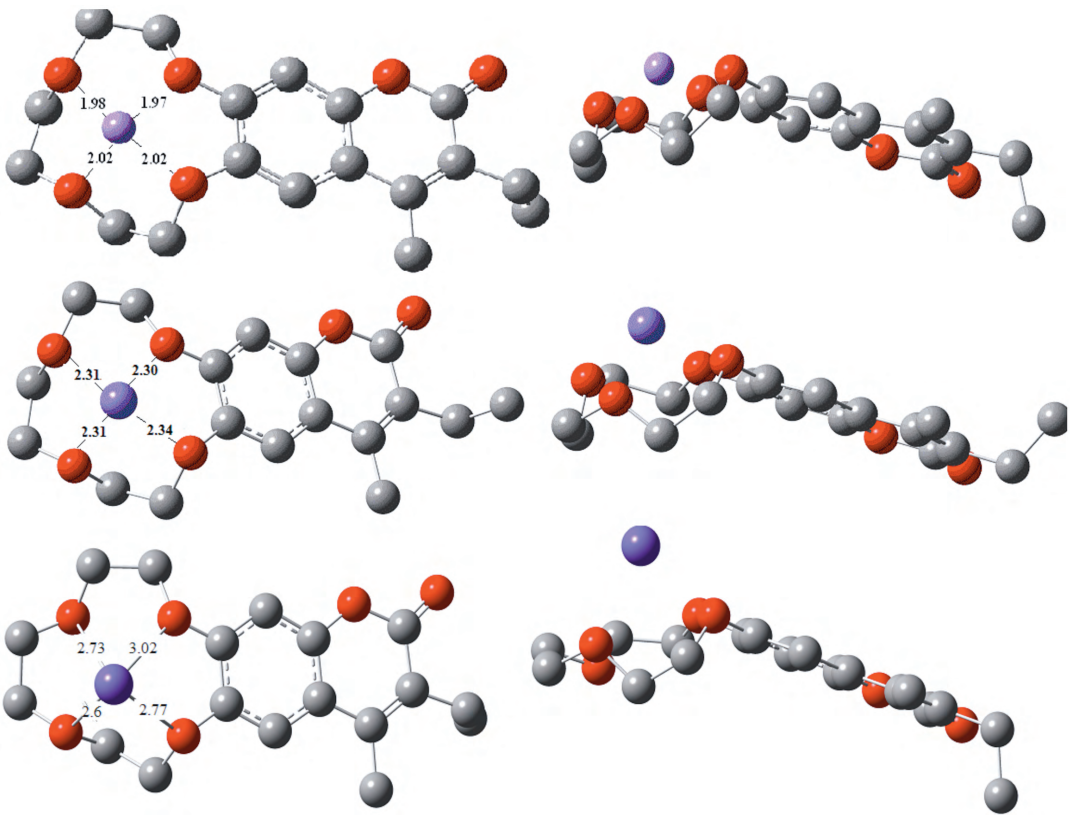

Figure 5. Front view (left) and side view (right) of $5aLi^+$ (top), $5aNa^+$ (middle), and $5aK^+$ (bottom).

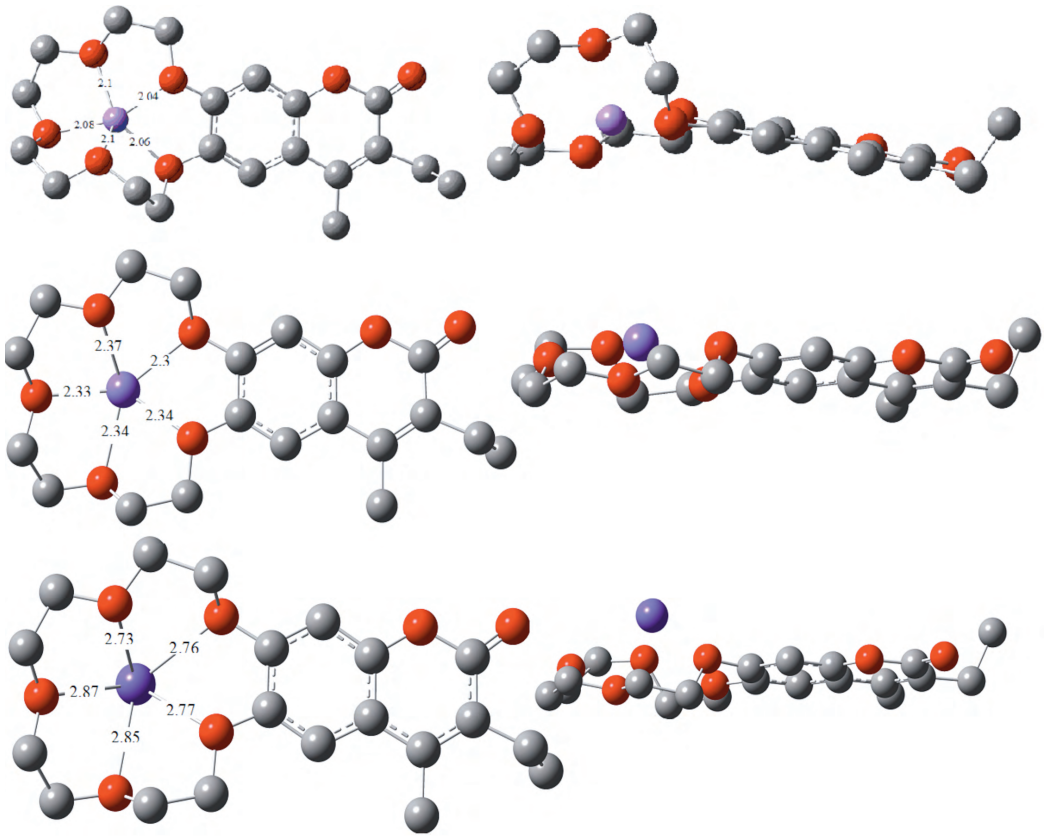

Figure 6. Front view (left) and side view (right) of $5bLi^+$ (top), $5bNa^+$ (middle), and $5bK^+$ (bottom).

Table 7. Comparison of the experimental (X-ray)[21] and theoretical (DFT) bond distances (in Å) for the M^+-O coordination bond in the $18c6Na^+$ and $18c6K^+$ complexes.

	Exp. (in Å)	This work (in Å)		Exp. (in Å)	This work (in Å)
Na...O(1)	2.6	2.6	K...O(1)	2.77	2.79
Na...O(4)	2.6	2.6	K...O(4)	2.81	2.81
Na...O(7)	2.5	2.6	K...O(7)	2.83	2.82

Although the charge transfer is not significant, it occurs to some extent between the metal ion and the negatively charged oxygen atoms of the crown-ether part of the molecule. We observed that when the geometrical fit between the size of the cations and the crown cavity gets better, the cations are accommodated better, and then a slight charge transfer of up to +0.14 esu from metal to oxygen atoms occurs (Table 8). If this is the case, the metals reside at the center of the crown ring with coordination to all oxygen atoms at large. Better coordination of the metal ion to the crown ether cavity is reflected in such a way that higher binding energies are obtained. The UV spectral shifts are also related to the electron density on the crown ether rings. Since the electron density in a neutral molecule is constant, when it increases in the crown moiety, it must decrease in the coumarin moiety, resulting in the blue shifts in the peaks belonging to $\pi - \pi^*$ transitions in the spectra.

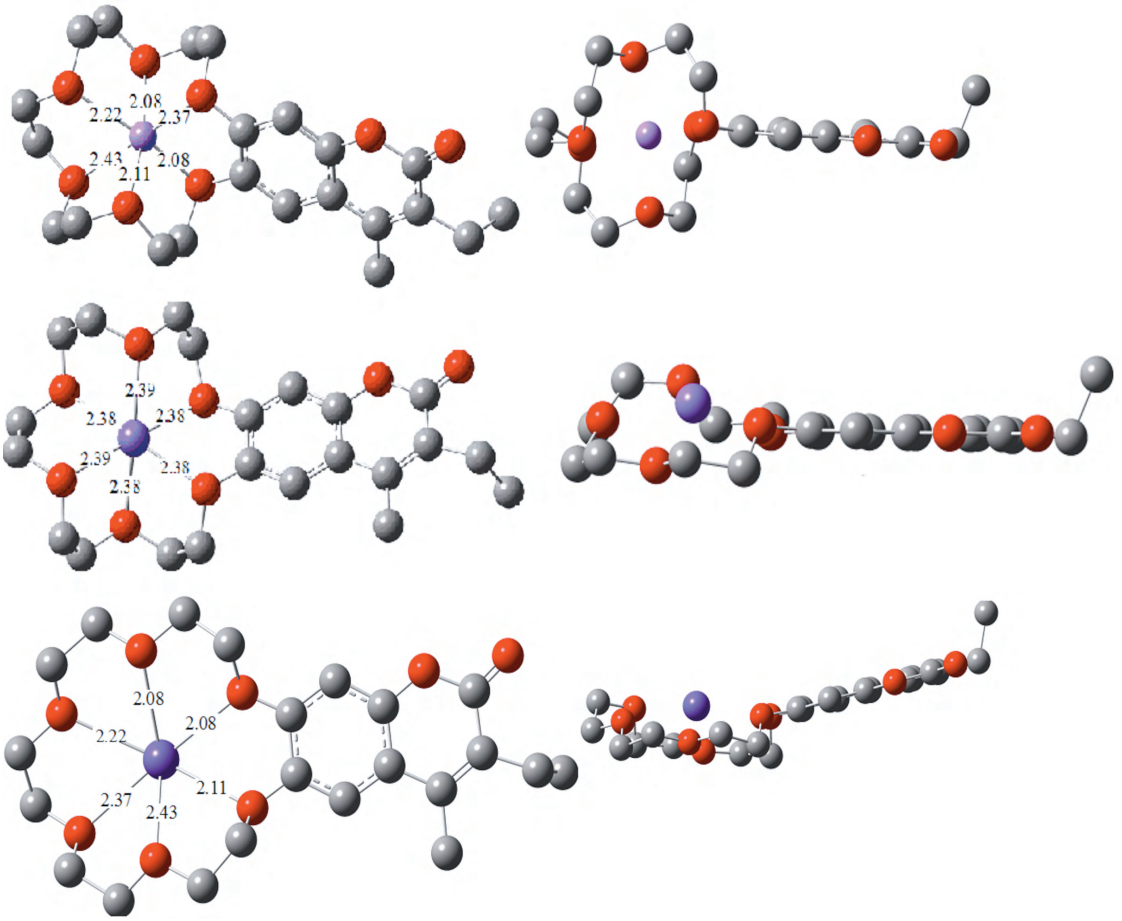

Figure 7. Front view (left) and side view (right) of $5cLi^+$ (top), $5cNa^+$ (middle), and $5cK^+$ (bottom).

Table 8. Charge on the metal ion in $(ML)^+$ complexes.

Molecule	Li	Na	K
5a	0.89	0.86	0.89
5b	0.95	0.92	0.92
5c	0.96	0.94	0.92
5d	0.86	0.86	0.89
5e	0.95	0.92	0.95
5f	0.96	0.94	0.92
6a	0.89	0.95	0.96
6b	0.87	0.94	0.94
6c	0.89	0.91	0.92
6d	0.86	0.95	0.96
6e	0.92	0.92	0.94
6f	0.89	0.91	0.92

Conclusion

In this study, DFT calculations at the B3LYP/6-31g+(d)//B3LYP/6-31g(d) level were performed to study the structural and optical properties and the cation selectivities of a series of coumarin-crown complexes. The geometric parameters of the optimized structures were tested with the X-ray data available in the literature. We showed that the incorporation of the coumarin part improved the optical properties significantly and thus enabled these complexes to absorb in the UV region. The peaks that appeared due to the coumarin were observed at around 300 nm, and the peaks observed for the naked crown ethers in the region of 140-160 nm shifted to a higher wavelength at around 190-220 nm. The maximum peak positions were affected by the type of the metal ion, the position of the coumarin attachment, and the type of the substituents in the coumarin moiety. The cation selectivity of the complexes, which depends on the size match between the metal ion and the crown ether cavity, the position of the coumarin ring, and the nature of the substituents, was studied by accurately determined bsse-corrected binding energies. Since there are many factors affecting the stability and the properties of such metal-bearing complexes, this study helps synthetic chemists to synthesize better complexes that are selectively sensitive to the impurities in solutions. The behavior of the complexes and kinetics of metal-binding reactions in aqueous media and also in different solvents will be studied by the explicit inclusion of the solvent molecules by computer simulations in future research.

References

1. Pedersen, C. J. *J. Am. Chem. Soc.* **1967**, *89*, 2495-2500.
2. Pedersen, C. J. *J. Am. Chem. Soc.* **1967**, *89*, 7017-7036.
3. Damewood, J. R.; Anderson, W. P.; Urban, J. J. *J. Comp. Chem.* **1988**, *9*, 111-124.
4. Erk, Ç. *Ind. Eng. Chem. Res.* **2000**, *39*, 3582-3588.
5. Blasius, E.; Cram, D. J.; Janzen, K. P.; Müller, W. M.; Sieger, H.; Trueblood, K. N.; Vögtle, F.; Weber, E. *Top. Curr. Chem.* **1981**, *98*, 1-189.
6. Gokel, G. *Crown Ethers and Cryptands*, Royal Society of Chemistry, Cambridge, 1991.
7. Regueiro-Figuero, M.; Esteban-Gomez, D.; Platas-Iglesias, C.; de Blas, A.; Rodriguez-Blas, T. *Eur. J. Inorg. Chem.* **2007**, *15*, 2198-2207.
8. Tiftikçi, E.; Erk, Ç. *J. Heterocyclic Chem.* **2004**, *41*, 867-871.
9. Bulut, M.; Erk, Ç.; Göçmen, A. *Pure Appl. Chem.* **1993**, *65*, 447-450.
10. Anderson, J. D. *J. Mass Spectrom.* **2003**, *227*, 63-76.
11. Islam, M. S.; Pethrick, R. A.; Pugh, D.; Wilson, M. J. *J. Chem. Soc. Faraday Trans.* **1997**, *93*, 387-392.
12. Stephens, P. J.; Devlin, F. J.; Chabalowski, C. F.; Frisch, M. J. *J. Phys. Chem.* **1994**, *98*, 11623-11627.
13. Stephens, P. J.; Devlin, F. J.; Ashvar, C. S.; Bak, K. L.; Taylor, P. R.; Frisch, M. J. *ACS Symposium Series* **1996**, *629*, 105-113.
14. Becke, A. D. *J. Chem. Phys.* **1993**, *98*, 5648-5652.
15. Passos, O.; Fernandes, P. A. *Theor. Chem. Acc.* **2011**, 119-129.

16. Frisch, M. J.; Pople, J. A. Gaussian 03, Revision B.05, Gaussian Inc., Pittsburgh, PA, USA, 2003.
17. Elik, M.; Serdaroğlu, G.; Özkan, R. *C. Ü. Fen-Edebiyat Fakültesi Fen Bilimleri Dergisi* **2007**, *28*, 53-65.
18. De Backer, M.; Hureau, M.; Depriester, M.; Deletoille, A.; Sargent, A. L.; Forshee, P. B.; Sibert, J. W. *J. Electroanal. Chem.* **2008**, *612*, 97-104.
19. Homem-de-Mello, P.; Mennucci, B.; Tomasi, J.; da Silva, A. B. F. *Theor. Chem. Acc.* **2005**, *113*, 274-280.
20. Tomasi, J.; Mennucci, B.; Cances, E. *J. Mol. Struct. (THEOCHEM)* **1999**, *464*, 211-226.
21. Dobler, M.; Dunitz, J. D.; Seiler, P. *Acta Cryst.* **1974**, *30*, 2741-2743.
22. Seiler, P.; Dobler, M. *Acta Cryst.* **1974**, *30*, 2744-2745.
23. Kaneko, F.; Sasaki, K.; Kashihara, N.; Okuyama, K. *Soft Materials* **2011**, *9*, 107-123.
24. Wilson, M. J.; Pethrick, R. A.; Pugh, D.; Islam, M. S. *J. Chem. Soc. Faraday Trans.* **1997**, *93*, 2097-2104.
25. Ali, Sk. M.; Maity, D. K.; De, S.; Shenoi, M. R. K. *Desalination* **2008,** *232*, 181-190.